

Four-Year On-Site Measurement of Heat Flow in Slab-on-Ground Floors with Wet Soils

Harold A. Trethowen, P.E.
Member ASHRAE

Angelo E. Delsante, Ph.D.

ABSTRACT

This paper outlines the methods and results of a four-year project that measured heat flows through two uninsulated slab-on-ground floors on nominally wet soils. One floor was on peat soil, the other on clay, and water table depths were 0.5 m to 1.0 m through most of the year. Heat fluxes were measured over the whole floor using heat flux transducers (HFT) at the concrete floor surface, and temperatures were measured by thermocouple, continuously for four years. The soil conductivities and soil temperatures were measured daily at 11 positions near one edge of the floors.

The R-values of these two floors can be calculated from ASHRAE or CIBSE Handbooks as $\sim 1.6 \text{ m}^2 \cdot ^\circ\text{C}/\text{W}$ and $1.3 \text{ m}^2 \cdot ^\circ\text{C}/\text{W}$. The floor R-values were measured, using a cumulative averaging method, to be $2.4 \text{ m}^2 \cdot ^\circ\text{C}/\text{W}$ and $1.0 \text{ m}^2 \cdot ^\circ\text{C}/\text{W}$, respectively, differing by about +50% and -25% from the calculated values. The measurement error is assessed as within $\sim \pm 7\%$. The measurements indicate that not only the soil conductivity but also the external wall thickness must be considered when determining floor performance. In the two houses in this project, the calculation errors attributable to not correcting for soil conductivity were $\sim +50\%$ and -10% , while those from not correcting for external wall thickness were $\sim +10\%$ and $+30\%$. The formulae developed by Delsante (1990) and improved by Davies (1993) best fitted the measurement.

Subsidiary data on edge temperature profiles, apparent distribution of R-values over the floor, and the sensitivity to indoor temperature fluctuations are also described. The influence of seasonal and short-term variations of indoor temperature are of practical significance, and the timing of floor heat flux rise and fall raises some questions about the contribution of the floor to overall heat losses.

INTRODUCTION

Objective and Background

Heat losses were measured in situ from two uninsulated slab-on-ground concrete floors on wet ground continuously over an extended period of four to five years. The main purposes of the project were to clarify uncertainties in the calculated values from handbook methods of calculation and to include the effects of wet soils, which are a common feature in the New Zealand winter. A final goal was to guide local building code methods for rating floors of this type. An interim paper on the project was given by Trethowen (1992).

A number of previous studies on this subject have been made, many by analytic methods or by computer modeling. At the commencement of this project, it was felt that the experimental support for this subject was weak. Previous measure-

ment studies have tended to be continued for too short a period (Ackerman and Dale 1987; Bareither et al. 1948; Dill et al. 1945) to permit an approach to an equilibrium cyclic state for the floors or have offered insufficient information on key factors such as soil conductivity (Spooner 1982). Most have been with relatively dry soils. The situation has improved since this project began, but long-term measurement studies are still sparse.

Most of the standard simplified calculation methods (Anderson 1990; ASHRAE 1972, 1993; CIBSE 1970; Davies 1993; Delsante 1990) are based on steady-state conditions. When these are applied to actual building heat losses, they require adjustment to allow for the nonachievement of equilibrium, but the measurement support base for any adjustment is also weak.

It had been generally accepted until about 1982 that the slab-on-ground component of space heating loss from houses

Harold A. Trethowen recently retired from the Building Research Association of New Zealand, Wellington, where he was senior research engineer. Angelo E. Delsante is principal research scientist in the Division of Building Construction, Engineering, CSIRO, Melbourne, Australia.

was well enough known, using handbooks such as ASHRAE (1993) and CIBSE (1970). Then work in the U.K. by Spooner (1982) suggested that the actual losses were perhaps half the then-current handbook values. This report was quickly accepted by concrete interests, although there was no satisfactory explanation for this result—the soil properties in particular were not recorded in that study.

Later work in the U.K. (ECD 1987; Everett et al. 1985) reported measuring nearly double the CIBSE-calculated heat losses and accounted for both this and Spooner's work by comparing the soil properties. The overall situation thus was that slab-on-ground floor R-values became uncertain within a range of 2:1, even after due allowance was made for climate and heating standard.

To give a clearer basis for building control decisions in New Zealand, there was deemed to be a need to demonstrate what heat losses would apply for the local climate and soil types. There was also perceived to be a need to include the effects of wet ground, which is a feature of the local winter climate. The effect of external wall thickness emerged only later as a factor. It had been routine to ignore this in engineering calculations, although it appears in all of the formulae.

Method

The project involved the determination of floor heat flows and temperatures by continuous automatic recording, along the general plan indicated in Figure 1. Indoor and outdoor temperatures were also recorded, as well as daily measurement of the soil thermal properties. Floor heat flows were measured in 14 zones over the whole floor by heat flux transducers (HFT). Later computer processing refined the results into usable heat loss coefficients, i.e., thermal resistances. The

method of measurement could be applied in any climate, and it is presumed that the ground resistance would vary only with soil and moisture conditions.

SITE DESCRIPTION

Houses

The two houses are referred to as "Paraparamu" and "Whitby" (sometimes abbreviated to "P" and "W") after the name of the suburban districts where they are located. Photographs of the houses are presented in Figures 2 and 3, and overall properties of the houses are listed in Tables 1 and 2. Both houses are free-standing, single-unit dwellings and were instrumented at the time of construction. Measurements commenced as soon as construction was completed. The houses were occupied throughout the project. Neither floor was insulated in either core or perimeter regions.

House plans are shown in Figures 4 and 5. The Paraparamu house (P) has a floor area of approximately 140 m², plus a small upper floor space not part of this study. It has masonry veneer external walls and is built on peat soil on long steel-rail piles. Floors were covered with slate in the conservatory (zones 8, 14) and carpeted elsewhere except for toilet and bathroom. The occupants were asked to maintain steady and uniform winter heating to about 20°C. This was done under the control of normal room thermostats, mostly by flued direct gas heating.

The Whitby house (W) has a floor area of 102 m², and the day room portion of this, 41 m², was instrumented for this study. It has one floor, timber-framed walls clad with coated cement fiberboard sheet, timber trussed roof with tiles. It is sited on clay soil, and the soil remains obviously wet from run-

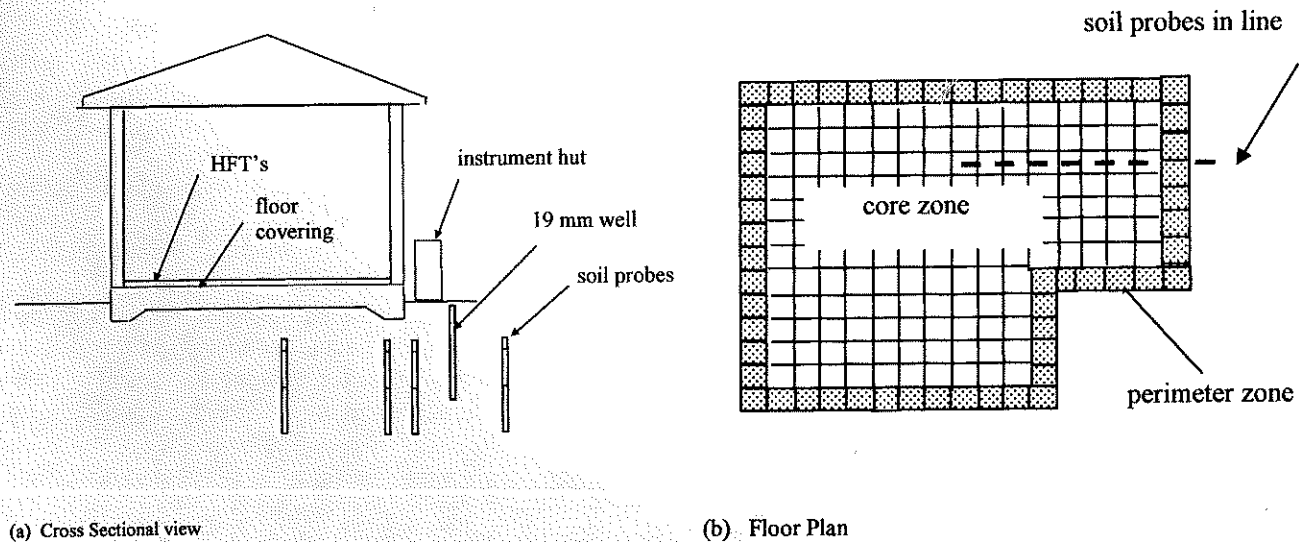


Figure 1 Outlining the measurement scheme. (a) Cross-sectional view, (b) floor plan.



Figure 2 Front view of Paraparaumu house during construction.



Figure 3 Front view of Whitby house during construction (note data logger hut at lower right).

off from a hillside above the site (to the right rear of Figure 3). Floors in the monitored area were carpeted, except for a tiny kitchenette. The occupants were asked to maintain steady and uniform winter heating to 20°C, and low-temperature electric heating was used.

Site Data

Typical soil conductivities are given in the *ASHRAE Handbook—Fundamentals*. The values in the 1972-1989 editions were found to roughly fit Equation 1:

$$k \sim k_0 \cdot (1 + 7m) \cdot (\rho_0/1600)^{2.1} \quad (1)$$

where

- k = conductivity, W/m·°C;
- m = moisture content by weight (0 to 1);
- ρ = bulk density, kg/m³.

The suffix 0 indicates value for dry soil

($k_0 = 0.5$ clay, $k_0 = 0.6$ loam, $k_0 = 0.9$ sand, $k_0 = 1.2$ quartz).

TABLE 1
General Details of the Two House

		Paraparaumu	Whitby
Perimeter floor area*	m ²	52.4	11.5
Core floor area*	m ²	89.3	29.5
Total floor area	m ²	141.7	41.0
Perimeter length	m	60.2	22.0
Perimeter wall thickness	m	0.27	0.10
Mean roof R-Value	m ² ·C/W	~ 2.2	~ 2.0
Mean wall R-Value	m ² ·°C/W	~2.0	~ 1.8

* Perimeter area is taken as within 1 or 1 HFT width of the floor edge, viz. 0.6 or 1.2 m.

Values in the 1993 edition approximate to Equation 2

$$\begin{aligned}
 k &\sim 0.7 + 0.05 \cdot m \text{ for fine grained soils,} \\
 &\sim 0.7 + 0.1 \cdot m \text{ for poorly graded soils,} \\
 &\sim 0.7 + 0.2 \cdot m \text{ for well graded soils.} \quad (2)
 \end{aligned}$$

Thus, the 1989 Handbook data indicate soil conductivity values of about 0.4 (P) and 1.8 (W), while for the 1993 Handbook these would be > 2 (P) and 1.3 (W). This is a large difference, and neither value is close to the measured values of 0.7 (P) and 1.1 (W).

Farouki (1986) provides a much more comprehensive source of data for soil conductivities. From Farouki it might be

TABLE 2
Derived Details of the Two Houses*

		Paraparaumu	Whitby
Derived soil conductivity k	W/m·°C	0.7	1.1
Derived soil diffusivity K	m ² /s	11×10^{-7}	7×10^{-7}
Soil density	kg/m ³	500-700	1200-1500
Soil moisture content (m.c.)	%	20-50	25-35
Mean temperature, indoors	°C	21.3	18.7
Mean temperature, outdoors,	°C	13.4	13.0
Mean heat flow, perimeter,	W	193	53.0
Mean heat flow, core,	W	128	45.2
Mean heat flow, total,	W	321	98.2
Mean heat flux, perimeter,	W/m ²	3.68	4.61
Mean heat flux, core,	W/m ²	1.43	1.53
Mean heat flux, total	W/m ²	2.27	2.40

* ~ half of the Whitby house is instrumented.

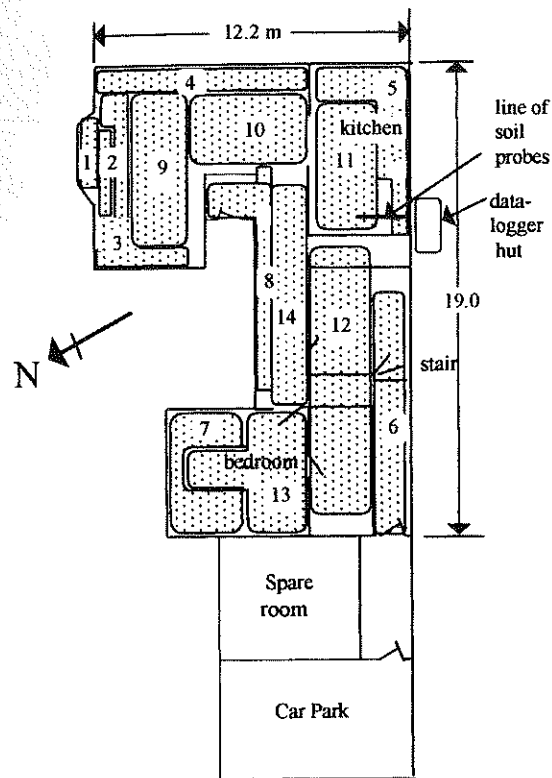


Figure 4 Floor zone layout of Paraparamu house ($N =$ equatorial side).

expected that the soil conductivity for the wet peat soil at Paraparamu would be below $1.0 \text{ W/m}\cdot\text{C}$ and possibly even below 0.5 depending on unknown factors such as the degree of peat formation and the type of minerals. The wet clay at Whitby might be expected to have conductivity anywhere between $0.5 \text{ W/m}\cdot\text{C}$ and $1.5 \text{ W/m}\cdot\text{C}$.

In view of the wide range of these expectations, it will be apparent that it will not be easy at present to confidently assign a thermal conductivity (k) value to the soil at the design stage of a building. Future measurement surveys may be desirable to reduce this problem.

Groundwater

On both sites the water table depth was permanently rather shallow. At Paraparamu, it ranged from $\sim 0.4 \text{ m}$ to 1 m with an apparent response to the rainfall in the previous few weeks. At Whitby, it ranged from 0.4 m to 0.6 m without an obvious response pattern. The Whitby site groundwater seems to be dominated by submerged runoff from a nearby hill, and the groundwater storage accumulation process may be too complex to be easily seen.

A point of interest in this project was whether annual convective exchange of water might be important. Would water dry or drain during summer, to be replaced by new water next winter? Preliminary estimates based on gross annual change in soil moisture from "saturation" to "wilt point" were

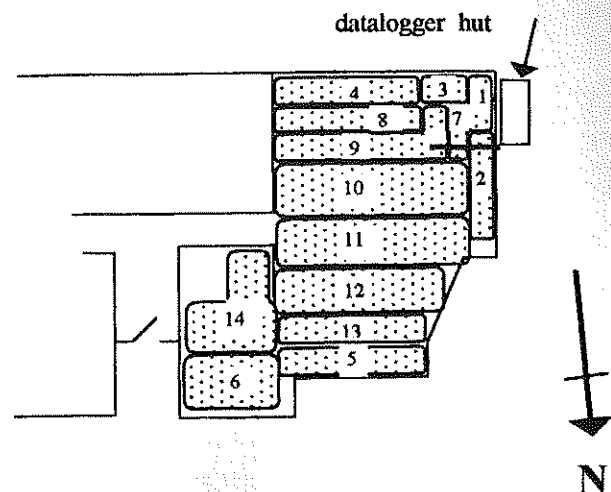


Figure 5 Floor zone layout of Whitby house ($N =$ equatorial side).

that this process could contribute to the heat flux by some 0.1 W/m^2 to 1.0 W/m^2 , which was expected to be significant but not dominant at these sites. In the event, neither ground moisture contents nor water table depth changed significantly with season, and so the associated heat flux would be small and was not pursued further.

INSTRUMENTATION

Floor Temperatures

The temperature sensors were copper/constantan thermocouples taped to the concrete surface of the floor. They were connected as differential thermocouples to indicate temperature relative to a reference block, whose absolute temperature was indicated by two embedded semiconductor transducers with 0.1°C resolution. The reference blocks were externally insulated solid aluminium blocks of about 50 mm total thickness. Indoor temperatures were measured similarly with thermocouples at $\sim 0.3 \text{ m}$ and $\sim 2 \text{ m}$ above floor level ("lo" and "hi" in Figures 8 and 10).

Heat Flux Transducers

Surface heat fluxes at the surface of the concrete floor were measured over the whole floor using heat flux transducers (HFTs) bonded to the floor with contact adhesive. The HFTs were $1.2 \text{ m} \times 1.2 \text{ m}$ (or $0.6 \text{ m} \times 1.2 \text{ m}$), hand built from 4.5 mm hardboard backed with 8 mm expanded polystyrene and fitted with 16 (or 8) pair thermopiles. There were ~ 150 HFTs on the P floor and ~ 40 HFTs on the W floor. The calibration coefficients of these HFTs were individually calibrated (see "Calibration"), and they had a thermal resistance of about $0.25 \text{ m}^2\cdot\text{C/W}$. A "jointless" design was used for the thermopiles incorporated in the HFTs to improve long-term reliability, as shown in Figure 6.

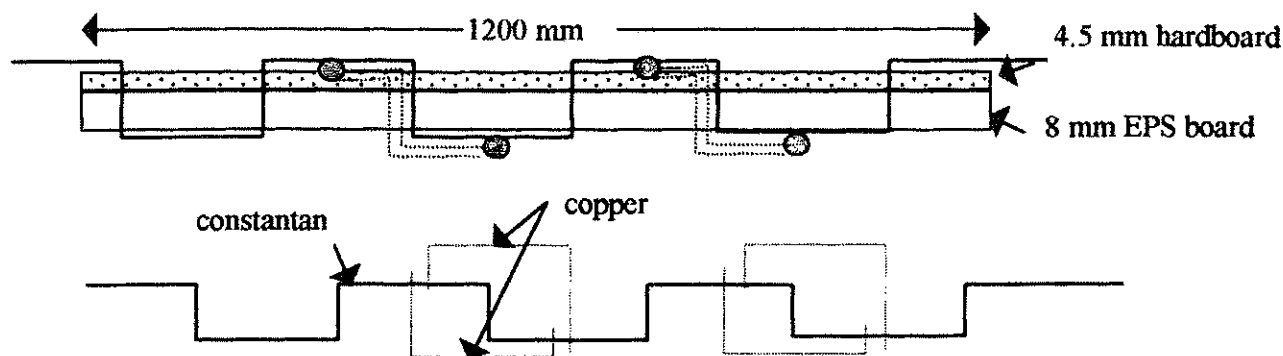


Figure 6 Method of thermopile wiring.

Failure of any one connection would produce no change in HFT calibration. Failure of a second joint has 97% probability of producing no change and a worst case outcome of changing calibration by 8%, without risk of losing continuity. Change of calibration from joint failure would be indicated by a change of electrical resistance, also of about 8%, or 1 ohm to 2 ohm in a total of 10 ohm to 30 ohm, depending on lead length. The electrical resistance of all HFTs was, therefore, monitored from time to time during the project, recording to ~ 0.1 ohm to detect any such changes, but none was observed.

Soil Temperature and Conductivity Probes

The thermal conductivity of the soil at various positions was measured using "needle probes," with about 7 mm diameter by 100 mm active heater length. These were built on 5 mm rigid glass fiber rods of 0.6 m to 3.0 m length. The needle probes contained a single thermocouple immediately under a nichrome tape heater coiled along the rod for soil temperature measurement and for monitoring temperature change after switch-on of the nichrome heaters during soil thermal conductivity measurement. The operating principle is described by Mulligan et al. (1985) and Carslaw and Jaeger (1959). A review of the reliability of this procedure is given by Farouki (1986), who comments that the method is probably the most reliable available for wet soils. The probe temperature rise was typically 2°C to 5°C , and it took 10 to 15 minutes for the measurement. The aim was to measure the soil conductivity once per day, and this aim was often, but not always, met.

CALIBRATION

Before installation, all HFTs were calibrated in a 1600 mm \times 1200 mm ASTM C236 guarded hot box rig. The HFTs were sandwiched in groups of three between 50 mm EPS insulating boards and guarded to force equal heat flux over the whole area. The calibration coefficients of the hand-made HFTs ranged from $5.6 \text{ W/m}^2 \cdot \text{mV}$ to $7.8 \text{ W/m}^2 \cdot \text{mV}$, with mean values of $6.34 \text{ W/m}^2 \cdot \text{mV}$ for full-size HFTs and $6.59 \text{ W/m}^2 \cdot \text{mV}$ for half-size HFTs.

The HFTs were installed by gluing them to the floor with contact adhesive to prevent movement and to provide a firm

footing. However, on completion of the project, the owner requested that the 15 HFTs in the conservatory area of the Paraparaumu house be removed. They had found the slightly flexible HFT base to be not rigid enough for the black slate floor tiles in that area.

We were able to recover 14 of these HFTs in apparently sound enough condition that their calibration could be rechecked. The average calibration of the 14 HFTs was within 7% of the original, but the calibration shift was noticeably greater on the more damaged HFTs (see Figure 7). The HFTs with little damage show small change in apparent calibration change, while those with more damage had larger changes. This indicates that the change in calibration was almost entirely due to damage at the time of removal and that the original calibration had been retained until that time.

RESULTS

Typical Hourly Heat Flux and Temperatures

A general outline of the conditions observed over the four years of observations are shown in Figures 8 through 11. These data are based on 10-day averages, chosen to reduce the

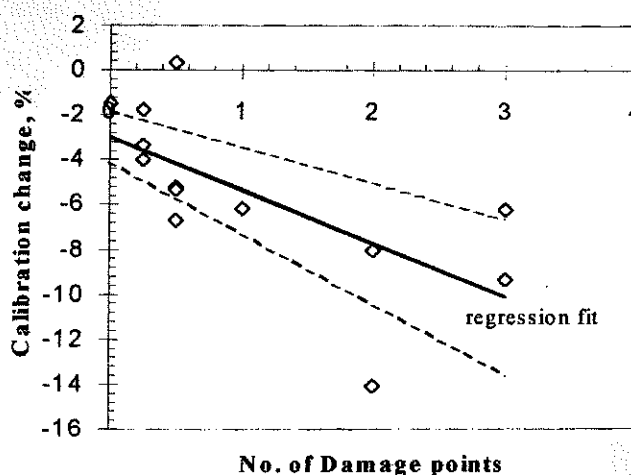


Figure 7 Final HFT calibration change vs. number of damage sites.

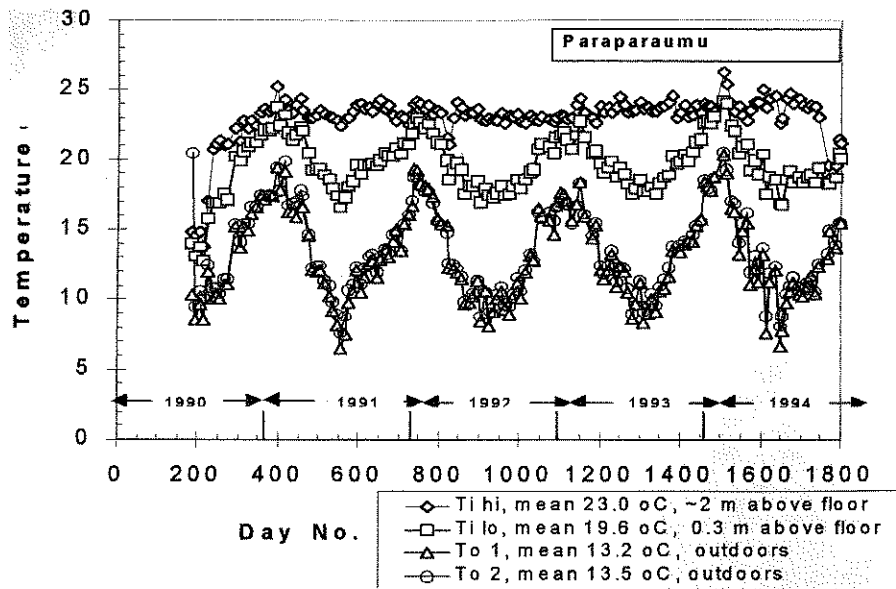


Figure 8 Temperatures in Paraparaumu house, 10-day average values.

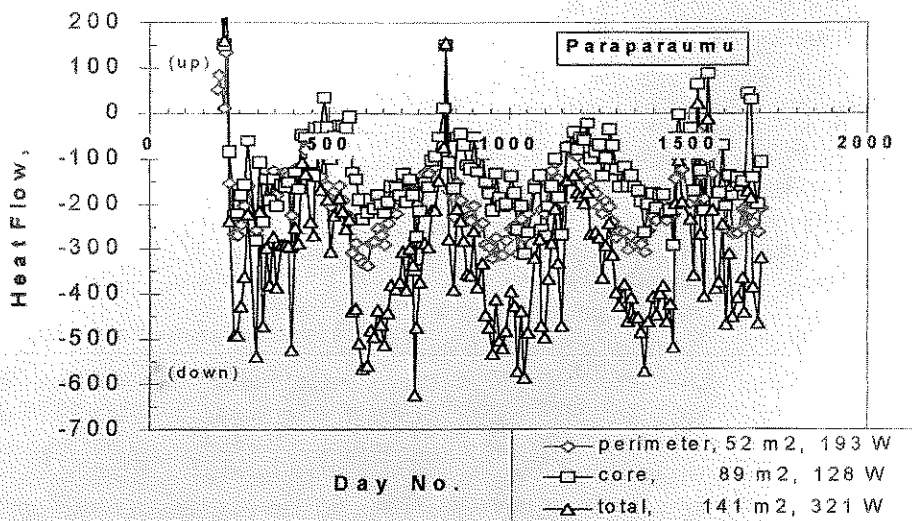


Figure 9 Core and perimeter area heat flows, Paraparaumu house, 10-day average values.

amount of data and to suppress daily swings and short-term weather fluctuations. Figures 8 and 10 show the indoor temperatures (“Ti hi” at 2 m and “Ti lo” at 0.3 m above the floor) and outdoor temperatures (“To”) at two different locations outdoors. Figures 9 and 11 show the corresponding floor heat flux values at the surface of the concrete floor. Positive values are for upward heat flow.

Figures 8 through 11 show several trends. Both outdoor and indoor floor temperatures lag some two months on the solar season. The floor heat flux lags more, four to six months. There was an apparent correlation between the floor heat flux and the rate of change of floor surface temperature—when the

floor surface temperature rises, the downward floor heat flux tends to increase, and vice versa. The average heat flux in the floor was not large, 2 to 5 W/m² downward, and there were no periods of sustained upward heat flux in any season. Over shorter periods of a week or less, there are some times when there are significant upward flows from the floor, but stored heat in the conservatory floor had only limited effect on the building’s heat energy flows, supplying less than 200 W to the building during times of peak discharge of stored floor heat (e.g., overnight). Figure 12 shows a typical 10-day, hour-by-hour record from one house in winter. This illustrates most of the behavior patterns seen in either house. There is a very

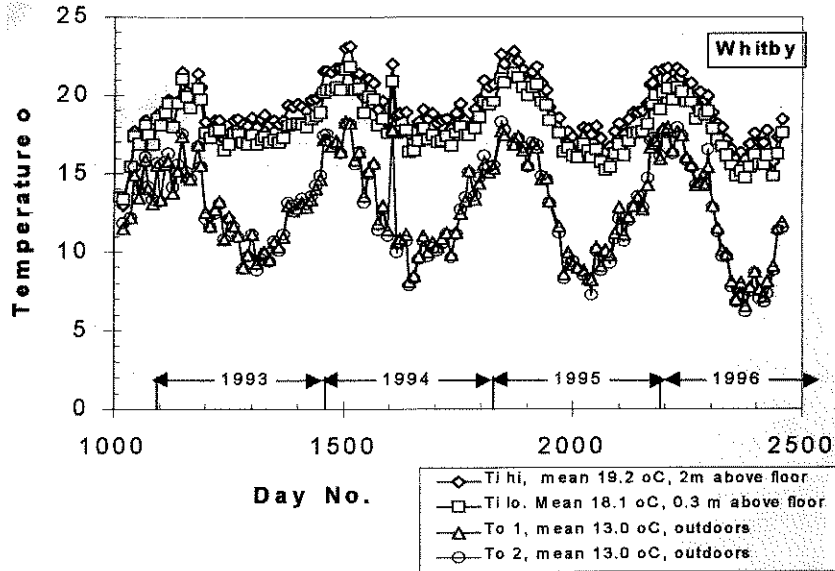


Figure 10 Floor temperatures and heat flux, Whitby house, 10-day average values.

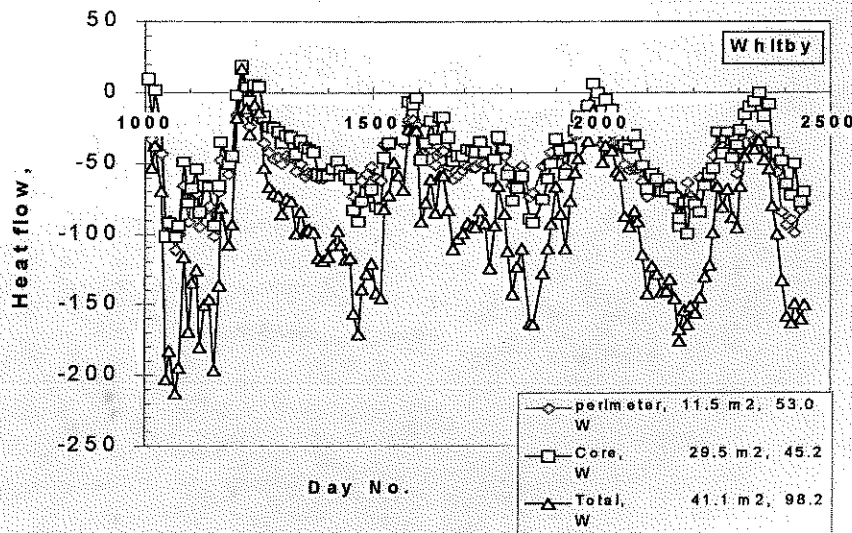


Figure 11 Floor heat flows, Whitby house, 10-day average values.

small daily fluctuation of concrete floor surface temperature, a phase reversal between outdoor air temperature and floor heat flux, and a less visible reverse correlation between rising floor temperature and downward heat flux. The typical physical sequence is that floors are warmed by sunshine in the morning, and an increased downward heat flux is a consequence of that change of temperature.

Cumulative R-Values

This section outlines the method for calculating the R-values of the various parts of the floor. The R-value is a steady-state property and refers to the long-term average heat flow resistance from indoors to outdoors, in this case for each part of the floor. Naturally, this resistance is low for edge zones and

becomes progressively larger for core regions. Core and perimeter zones are treated in the same way, as heat can only be "lost" to outdoors. Downward heat flow into the ground can only be stored, and this produces important dynamic effects, but these are not dealt with in this paper.

The R-value (R_n) for each zone was calculated by a progressive cumulative method in Equation 3a, from successive values of floor heat flux (q), floor surface (T_f), and outdoor temperatures (T_o), and these zone values are listed in Tables 3 and 4. Figure 13 shows the manner in which R_n from Equation 3a converges for 5 of the 14 zones of one floor.

$$R_n = \sum ((T_f - T_o) / q) \quad (3a)$$

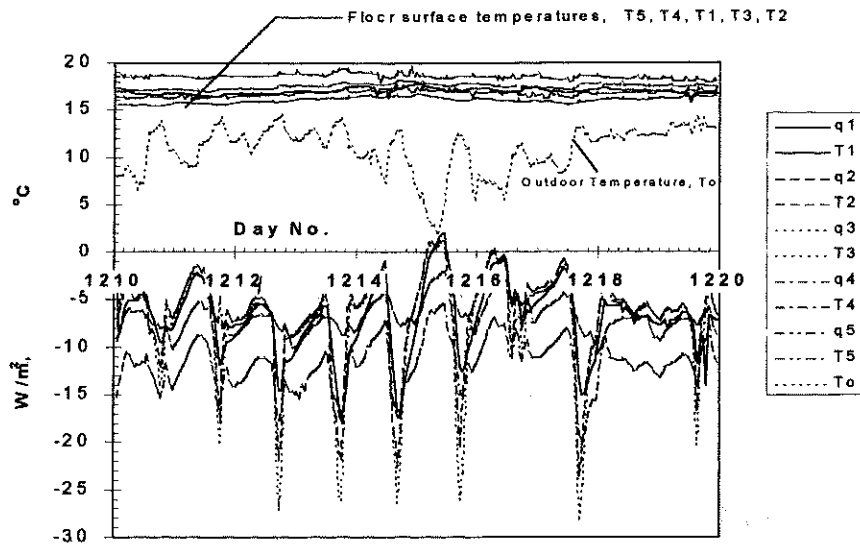


Figure 12 Typical daily variation, Paraparaumu house, winter 1991.

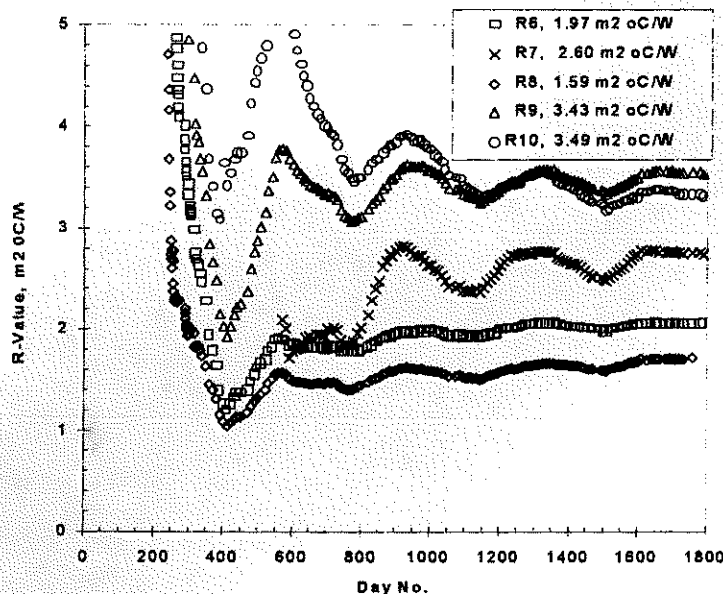


Figure 13 Cumulative floor R-values, Paraparaumu

The “whole floor” average R-values (R_{av}) are derived from the R_n values by area weighting, calculated using Equation 3b, and these are also listed in Tables 3 and 4. For each floor zone (area A_n), and each 1°C of indoor-outdoor temperature difference, the mean heat flow q is

$$q = A_n / R_n$$

where, over the whole floor, $\Sigma q = \Sigma (A_n / R_n)$ and also $\Sigma q = \Sigma (A_n) / R_{av}$ and

$$R_{av} = \Sigma (A_n) / \Sigma (A_n / R_n) \quad (3b)$$

In Figure 13, zones 6 through 8 are near the edge and have lower R than the core zones 9 and 10. Zones 6 and 7 are 1.2 m wide and zone 8 is 0.6 m wide. The R-values converge steadily

after an initial erratic period, with clear annual oscillations that fade in one to two years for perimeter regions but not until three years or more for core regions. The measurement time required was, thus, one to two years for the perimeter regions and about three years for the core regions. In the other edge zones 1 through 5, the R-value is lower for 0.6 m wide zones than for 1.2 m wide zones, and core zones tend to have rather higher R-values than edge zones.

The “measured” R-values in Tables 3 and 4 do not include the indoor surface coefficient or floor covering and apply between concrete floor surface and outdoors. Therefore an “adjusted” value for the R-value of the house P floor is also shown, adjusted for the contribution of carpet + indoor surface, i.e., $\sim 0.5 \text{ m}^2 \cdot ^\circ\text{C}/\text{W}$ over carpet, $0.2 \text{ m}^2 \cdot ^\circ\text{C}/\text{W}$ without carpet.

TABLE 3
Measured R-Values for Floor,
Paraparaumu House

Zone Number See Fig. 4	Zone Areas m ²	Measured R-Value See Fig. 13	Adjusted R-Value m ² ·°C/W
1	1.34	1.58	2.08
2	1.71	1.65	2.15
3	7.62	1.29	1.79
4	5.16	0.78	1.28
5*	9.84	0.94	1.14
6*	11.72	1.97	2.17
7	7.98	2.60	3.10
8*	7.02	1.59	1.79
9	15.34	3.43	3.93
10	13.00	3.49	3.99
11*	11.7	3.28	3.48
12*	24.25	4.56	4.76
13	12.24	5.60	6.10
14*	12.76	4.52	4.72
Whole Floor	142.6	2.35	2.80

* These positions have no carpet.
Boxed areas 1 through 8 are perimeter regions.

The distribution of R-value contours for house P was normal to edges, as expected, but for house W was decidedly skew, as shown in Figure 14. It has a general feature of being displaced toward the lower (N) portion of the floor. This skew is attributed to groundwater movement. The groundwater table depth is only 400 mm to 600 mm below ground level throughout the year, and groundwater is believed to flow from the top (S) or top right corner (SW). From the degree of asymmetry in Figure 14, it appears that the mean groundwater flow rate might be some 2 m per year.

TEMPERATURE GRADIENTS AT FLOOR EDGE

The mathematical derivations of the floor formulae define an edge temperature gradient from inside to outside temperature, and this is taken as over the actual external wall thickness. But the mean edge temperature gradients here were not as steep as this. The floor edge temperature gradient actually occurred over a distance of more than a meter in both these houses, even though the wall thickness in one case was 270 mm and in the other about 100 mm. Values shown in Figures 16 and 17 are from house P, but both houses showed very similar behavior. Figure 16 shows 10-day average profiles for several periods between late summer and midwinter. It is clear that the edge

TABLE 4
Measured R-Values for Floor,
Whitby House*

Zone Number See Fig. 5.	Zone Areas m ²	Measured R-Value m ² ·°C/W	Adjusted R-Value m ² ·°C/W
1	0.72	0.26	0.76
2	1.80	0.40	0.90
3	0.72	0.40	0.40
4	2.16	0.34	0.84
5	2.52	0.59	1.09
6	2.88	2.02	2.52
7	0.72	0.59	1.09
8	2.16	0.52	1.02
9	2.88	0.59	1.09
10	5.76	1.85	2.35
11	5.76	2.43	2.93
12	5.04	3.17	3.67
13	2.16	2.04	2.54
14	5.76	2.67	3.17
Whole Floor	41.04	0.98	1.76

* Boxed areas 1 through 7 are perimeter regions.

temperature gradients extend over a distance far greater than the actual wall thickness. Nevertheless, the use of actual wall thickness in Equation 4 produced a satisfactory agreement with the measured result. This can be seen even more clearly in Figure 17, which shows the approximate edge temperature profiles over one day. There is a phase reversal between the exterior and ~ 600 mm from footing, indicating an apparent phase velocity of some 50 mm/h. It can also be seen in Figures 16 and 17 that the peak temperature gradient is not grossly different from what might have been obtained by compressing the total temperature difference into the nominal wall thickness.

DISCUSSION

The R-values measured here differ from estimates using the standard handbooks. The main reasons for this are attributed to the effects of (1) actual soil conductivity and (2) external wall thickness, which are not included in typical calculations, although they are required for all the standard formulae.

Of all the well-known formulae for slab floors (Macey 1949; Latta and Boileau 1969; Spooner 1982; Anderson 1990), the best fit in this case was found to be the Delsante/Davies formula (Davies 1993; Delsante 1990). This formula avoids asymmetry between the length and breadth of a rect-

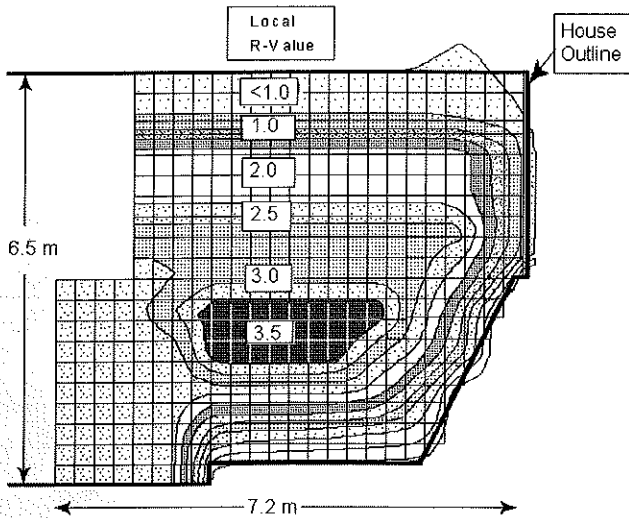


Figure 14 Map of R-values over the floor area, Whitby.

angular floor. The formula can be expressed as functions of area and perimeter, as in Equation 4 and 4a, and illustrated in Figure 15.

$$R = ((\pi \cdot A) / (k \cdot P)) / \ln\{(1 + x)(1 + 1/x)^x\}, \text{ m}^2 \cdot \text{C/W}, \quad (4)$$

where

$$x = (2 \cdot A) / (t \cdot P) = 1 \cdot d / t(1 + d), \quad (4a)$$

where

- d = half-width of floor (m),
- A = floor area (m^2),
- l = half-length of floor (m),
- P = floor perimeter (m),
- t = thickness of external walls (m),

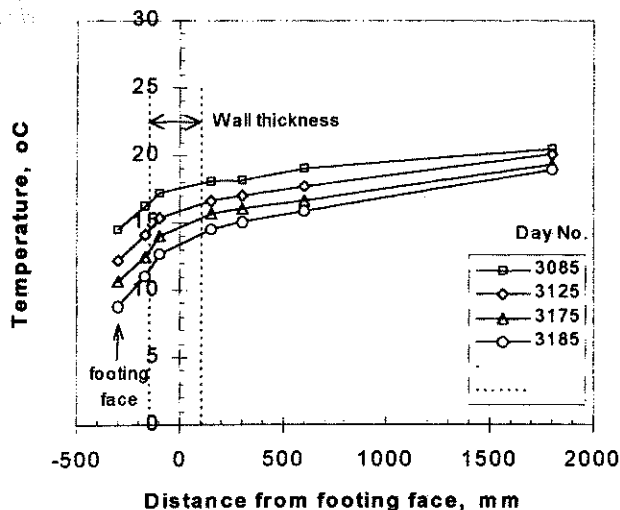


Figure 16 Edge temperature profile, Paraparamu house, 10-day averages

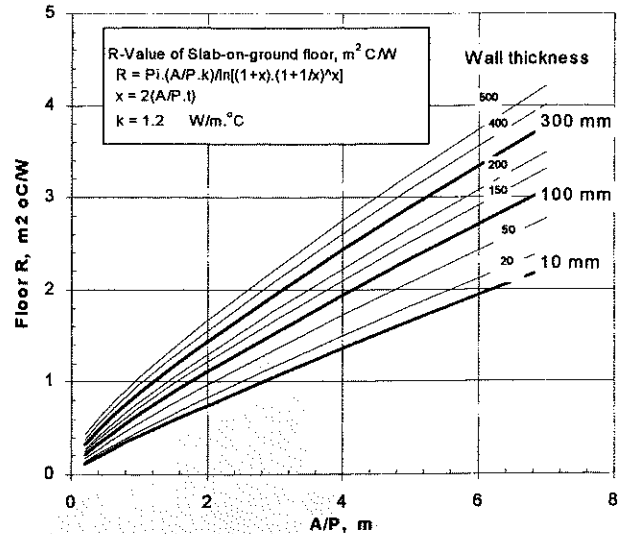


Figure 15 Thermal resistance of the ground by Delsante/Davies formula

k = soil conductivity ($\text{W/m} \cdot \text{C}$).

Equation 4 indicates that the thickness of the external wall is expected to have a very significant influence on the floor thermal resistance. Macey's formula and the ASHRAE method also include wall thickness terms. Physically this must arise from the fact that the heat flow can only escape by passing to the outdoors; if the wall is thicker, the path is longer, and the longer this path is, the less must be the heat flow.

Table 5 compares the measured R-values from this project with the values that would have been predicted from previous formulae. In Table 5, it is evident that agreement between measured and uncorrected calculated values is poor, but that adjustment for the real soil conductivity improves the

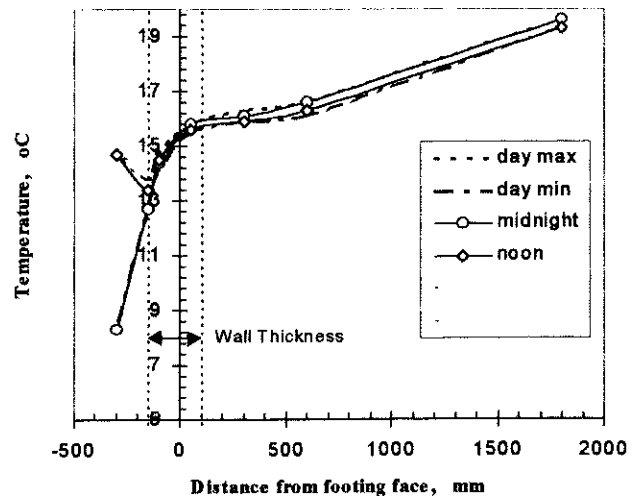


Figure 17 Edge temperature profiles over one day, Paraparamu house, day 3205. The two traces indicate the approximate limits of the day swing. (Note the difference in phase between outdoor and indoor).

TABLE 5
Summary of Calculated and Measured R-Values for Both Floors*

	Calculation Source				
	CIBSE	ASHRAE	Anderson	Delsante/Davies	Measured
Paraparaumu					2.35
"Normal"	1.6	1.7	1.55	1.4	
Adjusted to $k = 0.7$	3.2	3.4	3.1	2.8	
Adjusted for wall "t" 0.27 m				2.7	
Whitby					0.98
"Normal"	1.3	1.4	1.35	1.25	
Adjusted to $k = 1.1$	1.6	1.8	1.7	1.6	
Adjusted for wall "t" 0.10 m				1.2	

* These values are from indoor concrete surface to outdoor ground surface. Calculations are carried out using A and P from Table 1, k from Table 2. The "normal" values mean "as normally calculated," i.e., for soil $k = 1.4$ and external wall thickness is 300 mm.

fit considerably. However, the fit is further improved substantially by including the usually neglected exterior wall thickness. Of the four formulae considered, the Delsante/Davies formula gives the best agreement with our measurements. None of these formulae includes any reference to groundwater content or to groundwater table depth, and so they have not been included here, since our interest was in determining how reliable were the standard available methods. Such an effect could be added, using sources such as Delsante (1993) to compute an additional heat loss component, and, of course, could be equally well applied to any calculation method.

Within the limits of this project, the only observed influences of groundwater were (a) its effect on the apparent local as-measured soil conductivity and (b) the lateral displacement of the heat flux contours in house W (Figure 14). This point could be a result of the rather limited movement of the groundwater table in this project.

A rough measure of the vertical heat flux in the veneer of house P suggested that at times there was substantial heat flux up or down the veneer. These measurements were not verified but indicated that perhaps 10% of the total floor heat loss could have been occurring via the veneer.

Assessment of Measurement Accuracy

The basic accuracy of the measurement of the R-values in this project is estimated as $\pm 7\%$. This is based on the effect of errors in heat flux q and surface temperatures T_s of the concrete floor and on the outdoor temperatures T_o in Equation 3a.

The accuracy of individual temperature measurements T_s and T_o is assessed as within 0.2°C , and there are $\sim 400,000$ observations. The calibration of the temperature detectors is rated as $\pm 0.1^\circ\text{C}$ and of the ADC unit as ± 10 micro V ($\sim 0.25^\circ\text{C}$ with thermocouple). The assessed overall uncertainty in mean outdoor temperatures is $\pm 0.4^\circ\text{C}$, while that of indoor mean

values is $\pm 0.1^\circ\text{C}$. This gives an uncertainty of $\sim 6\%$ in the mean temperature difference of 8.0°C .

The heat flux meters were calibrated to within $\sim 3\%$, and there is evidence that this calibration quality was maintained throughout the project (see "Calibration" and Figure 7). The mean heat flux was $\sim 3 \text{ W/m}^2$, corresponding to a mean signal level of ~ 500 micro V. The mean ADC uncertainty of 10 micro V thus represents a mean error of 0.2% in the measurement of the HFTs, to be added to their calibration uncertainty of 3%. This leaves the heat flux measurement uncertainty at close to $\pm 3\%$.

The R-value derivation uses the temperature difference and the heat flux mean values and is itself subject to an uncertainty in the mean value of the reducing annual cyclic value of thermal resistance derived from the cumulative averaging process. The maximum potential error from this source is estimated as $\sim 2\%$. Thus, the total error in the measured R-value calculated from these values using the RMS method is that overall error = $(0.06^2 + 0.03^2 + 0.02^2) = 0.07$, or $\sim 7\%$.

An exception applies in zones 4 and 7 in the P house, where specific errors occurred, mainly during the first year, from cable or sensor failure and may have larger, uncertain, error (especially 7). Open circuit readings and electrical noise lead to initially large R-value errors. Zone 7 had particularly difficult wiring conditions, and almost half of its HFTs had to eventually be disconnected. Zone 4 had just a single failure, but it took some time to detect and repair. It was symptomatic in the calculations for these two channels that before correction both were highly sensitive to the starting point used in evaluating Equation 3a. When reanalyzed without these errors, whether by deleting the faulty time blocks or by substituting "borrowed" data from adjacent similar zones, both the result anomalies and the sensitivity disappeared. All other zones showed little response to the choice of starting point or to the introduction of a large disturbance partway into the calculation of Equation 3a.

CONCLUSIONS

The nature of a (nominally) five-year field study on heat flows in two uninsulated slab-on-ground floors on wet soils has been described. The results indicate the following.

- The thermal resistances of the two floors have been measured as $R\ 2.4\ \text{m}^2\cdot\text{C}/\text{W}$ for the P house and $1.0\ \text{m}^2\cdot\text{C}/\text{W}$ for the W house to within an estimated error of 7% for most zones. These compare with CIBSE (1970) calculated values of $R\ 1.6\ \text{m}^2\cdot\text{C}/\text{W}$ and $R\ 1.3\ \text{m}^2\cdot\text{C}/\text{W}$ for "standard" conditions ($k = 1.4$, $t = 300\ \text{mm}$). Values calculated from the Delsante/Davies formula, including actual soil conductivity and actual external wall thickness, are $2.7\ \text{m}^2\cdot\text{C}/\text{W}$ and $1.2\ \text{m}^2\cdot\text{C}/\text{W}$, respectively. The measurement time required was about one year for the perimeter regions and about three years for the core regions, when calculated using a cumulative averaging method.
- Thermal conductivity of wet peat soil at site P varied over $0.6\ \text{W}/\text{m}\cdot\text{C}$ to $0.9\ \text{W}/\text{m}\cdot\text{C}$, with a mean value calculated as $0.7\ \text{W}/\text{m}\cdot\text{C}$. Thermal conductivity of wet clay soil at site W varied over $0.9\ \text{W}/\text{m}\cdot\text{C}$ to $1.5\ \text{W}/\text{m}\cdot\text{C}$, with a mean value calculated as $1.2\ \text{W}/\text{m}\cdot\text{C}$. These contrast with handbooks, which commonly use a value of $1.4\ \text{W}/\text{m}\cdot\text{C}$, although many handbooks do not make this clear. That omission seems to be taken as a defacto indication that soil conductivity is unimportant or does not vary much. In this project, the effect of groundwater appeared to be via the apparent soil conductivity as measured in situ rather than by any more complex process involving the groundwater.
- Of the various formulae for manual calculation of floor thermal resistance, the recent formula from Delsante and Davies (Equation 4) gave better predictions than other well-known formulae such as those of Macey (CIBSE), Latta and Boileau (ASHRAE), and Anderson (BRE). One of the reasons is that the thickness of the external wall is retained as a more obvious parameter in the Delsante/Davies formula but has tended to become suppressed in others.
- The main part of floor heat loss takes place from the perimeter region, particularly the outer 0.5 m. Average heat flux over the outer 1.0 m was noticeably less than that over the outer 0.5 m and in core areas was even less. This is in distinct contrast to the results of Spooner, which suggested that the edge effect was weak.
- Heat flux at the concrete surface reached peak values of $-25\ \text{W}/\text{m}^2$ to $-30\ \text{W}/\text{m}^2$ (i.e., downward) in response to sunshine and $+10\ \text{W}/\text{m}^2$ (i.e., upward) at night. Both peak and average values were similar for both the conservatory and normal living space areas of comparable aspect. For the whole conservatory area of around $15\ \text{m}^2$, floor storage contributed less than 200 W to nighttime heating of the house.
- There were indications of a significant heat flow up and down the veneer part of the walls in house P, perhaps as

much as 10% of the total floor heat loss.

- Calculation of floor heat flows could be improved by using a two-stage process. It is not possible to represent the slow-response dynamic behavior of ground with a simple steady-state model. The annual average value should first be estimated from annual mean temperatures and the R-value as in present methods. A seasonal adjustment should then be superimposed on this to represent the annual pattern. For at least this project, this adjustment would be a very simple one, expressible as a fraction of the annual average loss.

ACKNOWLEDGMENTS

Acknowledgements are due to the New Zealand Foundation for Research Science and Technology Public Good Science Fund and the Building Research Levy for supporting this work.

REFERENCES

- Anderson, B. 1990. The U-value of ground floors: Application to building regulations. BRE Information Paper IP3/90. Building Research Establishment, Garston.
- ASHRAE. 1972-1993. *ASHRAE Handbook—Fundamentals*. Atlanta: American Society of Heating, Refrigerating and Air-Conditioning Engineers, Inc.
- Carslaw and Jaeger. 1959. *Conduction of heat in solids*, pp. 334, 345. Oxford: Clarendon Press.
- CIBSE. 1970. *Guide Book A*. London: Chartered Institute for Building Services.
- Davies, M.G. 1993. Heat loss from a solid floor: A new formula. *Building Services Engineering Research and Technology*. 14 (2): 71-75.
- Delsante, A.E. 1990. Theoretical calculations of the steady state heat losses through a slab-on-ground floor. *Building and Environment*, 25 (1): 25-31.
- Delsante, A.E. 1988. A comparison between measured and calculated heat losses through a slab-on-ground floor. *Building and Environment*, 23 (1): 11-17.
- Delsante, A.E. 1993. The effect of water table depth on steady state heat transfer through a slab-on-ground floor. *Building and Environment*, 28 (3): 369-372.
- ECD Partnership. 1987. Ground floor insulation. *Building Technical File*, No. 18, pp. 37-39.
- Everett, R., A. Horton, J. Daggart, and J. Willoughby. 1985. Linford low energy houses. Open University Energy Research Group, Report ERG50 ETSU-S-1025.
- Farouki, O.T. 1986. *Thermal properties of soils*. Transtech Publications, Germany.
- Latta and Boileau. 1969. Heat losses from house basements. *Canadian Building*, 19 (10).
- Macey, H.H. 1949. Heat loss through a solid floor. *Journal of the Institute of Fuel*, Oct., pp. 369-371.
- Mulligan, J.C., J.A. Edwards, R.R. Johnson, and G. Reddy. 1985. *Development of a probe for in-situ measurement*

of the thermal properties of earth in the vicinity of an earth coil. CLIMA 2000, Copenhagen, pp. 631-636.

- Spooner, D.C. 1982. Heat losses from an unoccupied house. Technical Report 549, Cement & Concrete Association, UK.
- Trethowen, H.A. 1992. A field study of heat loss of a slab floor and conservatory. PLEA Conference, Auckland. Also available as BRANZ Reprint No. 18.

MEASUREMENT STUDIES

- Ackerman, M., and J.D. Dale. 1987. Measurement and prediction of insulated and uninsulated basement wall heat losses in a heating climate. *ASHRAE Transactions*. 93(1): 897-908.
- Bareither, H.D., A.N. Fleming, and B.E. Albery. 1948. Temperature and heat loss characteristics of concrete floors laid on the ground. University of Illinois Small Homes Council.
- Dill, R.S., W.C. Robinson, and H.E. Robinson. 1945. Measurements of heat losses from slab floors. U.S. Department of Commerce, BMS 103.
- Everett, R, A. Horton, J. Doggart, and J. Willoughby. Linford low energy houses. 1985. Open University Energy Research Group, Report ERG50 ETSU-S-1025.
- Spooner, D.C. 1982. Heat losses from an unoccupied house. Technical Report 549, Cement & Concrete Association, U.K.
- Thomas, H.R., S.Q.W. Rees, and R.M. Lloyd. 1996. Measured heat losses through a real ground floor slab. *Building Research and Information*, 24 (1): 15-26.

BIBLIOGRAPHY

- Bahnfleth, W. P. 1991. Three dimensional modelling of heat transfer from slab floors. USACERL Technical Manuscript E89/11, CRREL.
- Billington, N.S. 1982. Heat loss through solid ground floors. *Journal of the Institution of Heating & Ventilation Engineers*, London. Part 1, Nov. 1951, pp. 357-370; Part 2, pp. 325-328.
- Delsante, A.E. 1988. Theoretical calculations of the steady state heat losses through a slab-on-ground floor. *Building and Environment*, 23 (1): 11-17.
- Delsante, A.E. 1983. Application of Fourier transforms to periodic heat flow into the ground under a building. *Int. J. Heat Mass Transfer* 26 (1): 121-132.
- Delsante, A.E. 1983. Modelling heat flow into the ground in program STEP. 4th International Symposium on the Use of Computers in Environmental Engineering Related to Buildings, Tokyo.
- Hagentoft, C.E. 1988. Heat loss to the ground from a building. Doctoral thesis, Lund Institute of Technology, Sweden.
- Jaques, R. 1997. Building thermal performance determination: A report of two houses. IPENZ Annual Conference, 1996. Available as BRANZ Conference Paper No. 33.
- Kusuda, T., O. Piet, and J.W. Bean. 1983. Annual variation of temperature field and heat transfer under heated ground surfaces. NBS Building Science Series, 156.
- DSIR. 1968. Soils of New Zealand, Part 3. Bulletin 26 (3), DSIR Soil Bureau, N.Z.
- Thomas, H.R., S.Q.W. Rees, and R.N. Lloyd. 1996. Measured heat losses through a real ground floor slab. *Building Research and Information* 24(1): 15-26.